Zhu *et al. Human Genomics* (2025) 19:27
https://doi.org/10.1186/s40246-025-00739-4

Human Genomics

RESEARCH Open Access

Dynamic profiling of Cell-free DNA fragmentation uncovers postprandial metabolic and immune alterations

Ziting Zhu[1], Tao Chen[2], Manting Zhang[1], Xiaodi Shi[1], Pan Yu[1], Jianai Liu[1], Xiuzhi Duan[1*], Zhihua Tao[1*] and Xuchu Wang[1*]

Abstract

Background Food intake affects body homeostasis and significantly changes circulating cell-free DNA (cfDNA). However, the source and elimination of postprandial cfDNA is difficult to trace, and it is unknown whether these changes can be revealed by cfDNA fragmentomics based on liquid biopsy.

Methods We performed shallow whole-genome sequencing of 30 plasma samples from 10 healthy individuals at fasting and postprandial (30-min and 2-h time points). We assessed the effect of postprandial states on cfDNA fragment size distribution and utilized deconvolutional analysis of end motifs to determine the potential roles of DNA nucleases in cfDNA fragmentation. We correlated the fragmentation index (defined as the ratio of short-to-long fragments) with gene expression to estimate the relative contribution of various cellular and tissue sources to cfDNA.

Results Compared to the fasting state, we observed a significant increase in short cfDNA fragments (70–150 bp) and a decrease in long fragments (151–250 bp) at the 30-minute postprandial state, followed by an inverse trend two hours later. Deconvolutional analysis of cfDNA end motifs showed that DNASE1L3 activity decreased at the 30-minute postprandial state, while DNASE1 and DFFB activities increased at the 2-hour postprandial state. We found that the expression of genes related to cellular metabolism and immune responses was upregulated at the postprandial state. Meanwhile, the contribution of cells and tissues involved in metabolic and immune progress to circulating plasma cfDNA was increased.

Conclusions The fragmentation of cfDNA is considerably influenced by postprandial states, highlighting the significance of taking postprandial effects into account when evaluating cfDNA as a biomarker. Furthermore, our study reveals the potential application of cfDNA fragmentation features in monitoring metabolic and immune status changes.

[†]Ziting Zhu and Tao Chen contributed equally to this work.

*Correspondence:
Xiuzhi Duan
duanxiuzhi@zju.edu.cn
Zhihua Tao
zrtzh@zju.edu.cn
Xuchu Wang
wangxc@zju.edu.cn

Full list of author information is available at the end of the article

Keywords Cell-free DNA, CfDNA fragmentation, Immune response, Metabolic process, Liquid biopsy, Postprandial effects

Background

Circulating cell-free DNA (cfDNA) composed of DNA fragments are shed from different tissues or cells via mechanisms such as apoptosis, necrosis, NETosis, or active secretion [1–4]. In 2015, Ivanov et al. first proposed the concept of "cfDNA fragmentomics" [5], which refers to the study of cfDNA fragmentation patterns to reveal its biological characteristics and clinical applications [6, 7]. The fragmentation of cfDNA is not a random event [5, 8]; it is intricately linked to nucleosome footprint, chromatin structure, gene expression, methylation status and nuclease activity in the tissue of origin [7, 9–15]. By assessing the fragmentation features across the entire genome, including fragment size, end motifs, preferred end coordinates, and jagged ends, cfDNA fragmentomics enhances the traditional liquid biopsy approach [16–22].

Prior reports suggested that the characteristics of cfDNA fragmentation exhibit notable stability, thereby underscoring the potential benefits of leveraging cfDNA fragmentomics in clinical settings. For example, Van der Pol et al. investigated the impact of several physiological and preanalytical variables on cfDNA fragmentation and found that the fragmentation profiles were mostly unaffected by the type of collection tubes, processing time, age, BMI, medications, and the presence of chronic conditions [23]. In addition, Hu et al. compared two centrifugation methods and observed no substantial differences in cfDNA fragmentomics, implying that these procedures do not significantly alter fragmentation profiles [24].

Food intake activates the innate immune system and causes a postprandial inflammatory response, which can be considered a physiological phenomenon [25, 26]. However, if the body is in a sustained immune system activation, it may induce chronic systemic low-grade inflammation. This status has been associated with the development of chronic diseases such as obesity, type 2 diabetes, cardiovascular disease and cancer [27–29]. The postprandial state leads to a decrease in the level of cfDNA concentration in plasma [30]. This change may reflect different biological processes such as apoptosis, necrosis or activation of immune cells. However, the source and clearance of postprandial cfDNA have yet to be studied in detail, and it is unknown how postprandial metabolic and immune changes affect cfDNA fragmentation characteristics.

In this work, we used cfDNA fragmentomics for the first time to assess postprandial metabolic and immune alterations. We focused on the dynamics of cfDNA fragmentation profiles in response to food intake. This factor is often overlooked but could have significant implications for the interpretation of liquid biopsy results. We hypothesized that the postprandial state, characterized by fluctuations in metabolic activity and immune response, may influence the release and processing of cfDNA, thereby affecting its fragmentation patterns.

Methods

Recruitment of healthy individuals

A cohort of 10 healthy adults were enrolled in our study, consisting of 5 males and 5 females. We excluded individuals who were younger than 20 years of age or older than 35 years of age; pregnant or breastfeeding women; those with a history of malignancy; subjects with a history of drug allergy; patients with chronic diseases, including diabetes mellitus, hypertension, and autoimmune disorders; individuals with a history of smoking or alcohol use; and those who had taken any medication in the 2 weeks before enrollment. We meticulously collected 10 ml of their blood at three distinct time points: at the fasting state, and at the 30-minute postprandial state and 2-hour postprandial state (as depicted in Fig. 1, Supplementary Table 1). For a more detailed overview of the study design, please refer to Supplementary Fig. 1. Participants were given a standardized meal (roughly 500–690 Kcal) and instructed to consume it around 8 am, finishing within 30 min. Participants were requested to rest for at least 30 min before collecting fasting blood samples and maintain a resting state throughout the study. The study protocol was approved by the Human Ethics Review Committee of the second affiliated hospital of Zhejiang University (2024LSYD0962), and written informed consent was obtained from all subjects before their involvement in the study by the tenets outlined in the Declaration of Helsinki.

Sample processing

Peripheral blood samples were collected into EDTA-containing tubes and centrifuged at 1,600 g for 10 min at 4 °C. The plasma was then further recentrifuged at 16,000 g for 10 min at 4 °C to pellet any residual cellular components and platelets. The plasma was stored at -80 °C for further use. We also reserved a portion of plasma samples for complete blood count (CBC), biochemical profiling (including liver and kidney function, electrolytes), insulin, and C-peptide testing, and recorded the relevant values (Supplementary Table 1). All procedures were completed within 2 h.

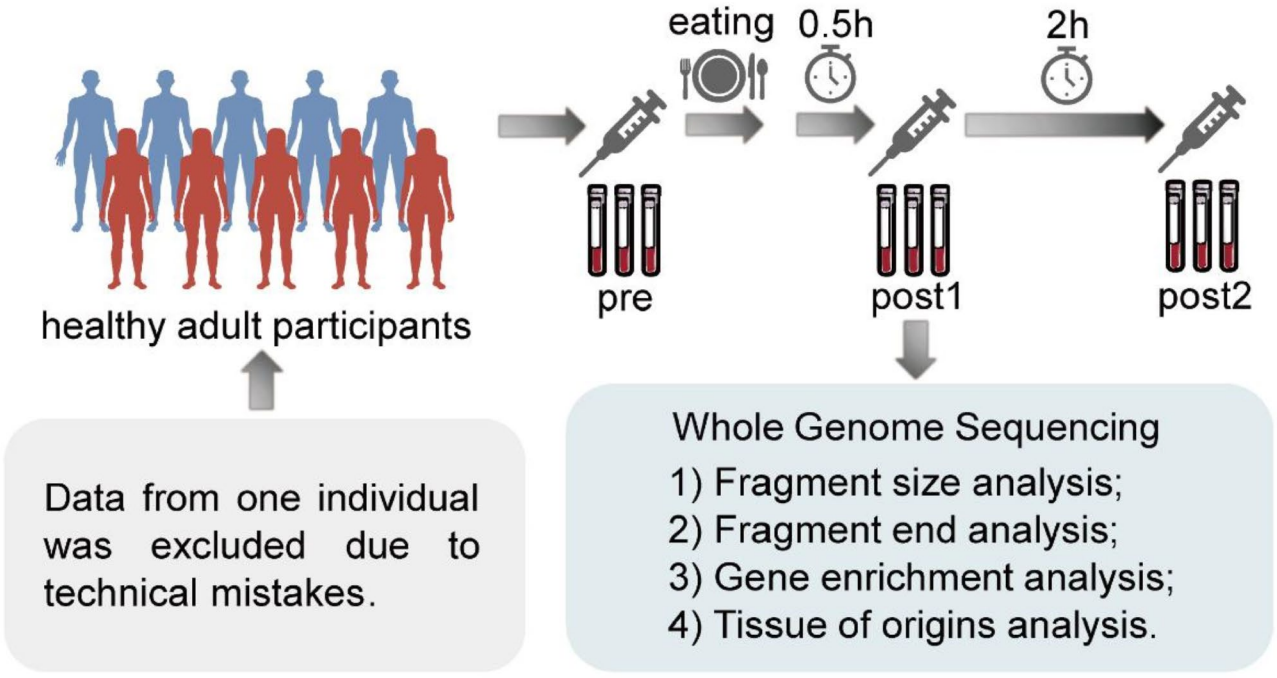

Fig. 1 Sample collection flowchart

CfDNA extraction and Whole-genome sequencing data processing

Cell-free DNA (cfDNA) was extracted from each plasma sample using the QIAamp Circulating Nucleic Acid Kit (Qiagen), in preparation for whole-genome sequencing at a depth of approximately 5× coverage. The cfDNA concentration was measured using a Qubit 3.0. Sequencing Libraries were prepared using 100 ng of cfDNA and the KAPA Hyper Prep Kit from Roche according to the manufacturer's instructions. Libraries quality was controlled using an Agilent 4200 TapeStation System (Supplementary Fig. 2). Paired-end sequencing was performed with a read length of 2 × 150 bp on the Illumina NovaSeq 6000 using S4 flowcells. Due to abnormal sequencing data, the data from one healthy subject was excluded. We preprocessed the raw data obtained from the Illumina sequencing platform using Fastp (https://github.com/OpenGene/fastp), which involved adapter trimming, removing reads with more than 5 consecutive N bases, eliminating reads with more than 40% low-quality bases (quality score ≤ 20), and applying sliding window trimming with a default window size of 4 bp and a quality threshold of 20. Sequencing reads were aligned to the reference genome (hg38) using Sentieon BWA (https://www.sentieon.com) with default parameters. To analyze the postprandial effects on fragment size distribution, we extracted cfDNA fragment sizes from BAM files using samtools (v.1.17). Short fragments were defined as those between 70 and 150 bp, while long fragments were defined as those with lengths between 151 and 250 bp. To estimate and control for the effects of GC content on sequencing coverage, we performed GC calibration for short fragments, long fragments, and the short-to-long fragment ratio following the protocol previously reported (https://github.com/cancer-genomics/delfi_scripts). We tiled the hg38 autosomes into 26,170 adjacent, non-overlapping 100-kb bins and calculated each bin's average fragment GC content. Scatter plots of average fragment GC versus coverage calculated for each 100-kb bin were generated using locally weighted scatterplot smoothing (LOESS) regression analysis (Supplementary Fig. 3). Plots were constructed in R (v.4.3.2) using the packages ggplot2 (v.3.5.1) and dplyr (v.1.1.4).

Deconvolutional analysis of CfDNA fragment end motifs

To further investigate the role of nucleases in cfDNA fragmentation, we conducted the deconvolution analysis of the end motif based on the method described by a previous study [31]. First, we calculated each sample's observed frequency (O) of 256 end motifs. Next, we used Python (v.3.8.10) to compute end motifs' expected frequency (E) based on the reference genome hg38. We defined the normalized end motif frequency as the ratio of observed to expected frequency (O/E) and divided by the sum of all 256 normalized motif frequencies. By integrating the six main cfDNA fragmentation patterns (F-profiles) identified in previous study [31], we performed the deconvolution analysis on the end motif frequencies of each sample using non-negative least squares (NNLS). This approach allowed us to determine

the contribution of each fragmentation pattern to cfDNA samples, thereby revealing the extent of these nucleases' involvement in the fragmentation process. The NNLS was implemented in R (v.4.3.2) using the package nnls (v.1.5).

Predicting gene expression using CfDNA fragmentation

We define fragmentation index as the GC corrected ratio of short to long cfDNA fragment proportions. To assess the relationship between fragmentation index and gene expression, we compared shallow WGS data from nine samples with gene expression data from the publicly available GEO dataset (GSM4182419). The correlation was further validated using deep WGS data (~200×) from a CUP (Cancer of Unknown Primary) patient (SAMN24592053) and matched peripheral blood mononuclear cell (PBMC) RNA sequencing data. The fragmentation index was utilized to estimate gene expression levels by applying a Gradient Boosting Machine (GBM) model. The GBM was implemented in R (v.4.3.2) using the package gbm (v2.2.2) with parameters: n.trees = 100, interaction.depth = 6, shrinkage = 0.1, train.fraction = 0.8, cv.folds = 5. To minimize additional confounding factors that result in systematic bias when studying the contributions of bulk gene expression on cfDNA fragmentation, we used the 5th and 95th percentiles of the housekeeping genes expression change distribution as thresholds for identifying differentially expressed genes (DEGs). The list of housekeeping genes used in this study can be found at https://www.tau.ac.il/~elieis/HKG/. Genes with predicted expression changes falling below the 5th percentile and above the 95th percentile of the housekeeping genes change distribution were classified as down-regulated and up-regulated DEGs. The DEGs were subsequently subjected to enrichment analysis using the clusterProfiler package (version 4.10.1) in R (version 4.3.2).

Estimating cell and tissue contributions

To study changes in postprandial plasma cfDNA from different cell or tissue types, we downloaded single-cell RNA sequencing data from the Human Protein Atlas (HPA) database (https://www.proteinatlas.org/about/download) and imported it into R (v.4.3.2) as a TSV file. We excluded cells from the reproductive system (e.g., spermatogonia, oocytes) and tissues (e.g., ovary, testis). We then correlated fragmentation index of each gene with the single-cell RNA-sequencing expression levels (nTPM) of these genes. We ranked 65 cell types and 51 tissue types based on the correlation strength and compared how the rankings of cells and tissues changed across three conditions: fasting, 30 min post-meal, and 2 h post-meal. Confidence intervals for correlations were obtained from 10,000 bootstrap repetitions with specificity fixed at 95%.

Statistics and reproducibility

Statistical analyses were conducted utilizing R version 4.3.2 and GraphPad Prism version 9.5.1. The normality of the data distribution was assessed using the Shapiro-Wilk test. Due to the small sample size, we chose the non-parametric Wilcoxon signed rank test to compare differences between multiple data sets. To control for the risk of Type I error due to multiple comparisons, we applied a Bonferroni correction to the significance level, which adjusted the significance level for each comparison to 0.05/3, i.e., approximately 0.0167. Thus, only results with $p < 0.0167$ were considered statistically significant. Correlations were assessed using Pearson (r) and Spearman (ρ) correlation coefficients. Permutational multivariate analysis of variance (PERMANOVA) was conducted using the R package vegan (version 2.6.10) to assess whether the principal components (PCs) differed significantly between groups. In analyzing changes in the relative contributions to cfDNA from various cells or tissues in samples before and after the meal, we constructed confidence intervals for correlations by 10,000 bootstrap replicates and set the specificity at 95%.

Results

Alterations in nuclease activity revealed by deconvolutional analysis of CfDNA end motifs

We first evaluated the plasma cfDNA concentrations as three timepoints: in the fasting state (pre), 30 min after the meal (post1), and 2 h after the meal (post2). The results showed a significant reduction in cfDNA concentration 30 min ($P = 0.0273$, paired Wilcoxon test) and 2 h after the meal ($P = 0.0195$, paired Wilcoxon test) compared with the fasting state (Supplementary Fig. 4A, Supplementary Table 1). These observations align with those of previous reports [30], that might be partially explained by the postprandial effect because the presence of lipids or proteins may interfere with DNA extraction yield from plasma (Supplementary Table 1). However, we did not find statistically significant associations when further analyzing the correlation between changes in cfDNA concentration and bilirubin, glucose, and triglyceride parameters (Supplementary Fig. 5). In addition, upon a closer inspection of the fragmentation distributions, even though the fragment size diversity (calculated as the normalized Shannon entropy index) was comparable between the fasting and postprandial states (Supplementary Fig. 4B), we observed a significant enrichment of short fragments following meal intake (Fig. 2A and B, Supplementary Table 2), which showed conflicts with the empirical expectation because the reduction in DNA extraction efficiency will primarily affects short fragments [32].

Given the alteration of cfDNA fragment size, we then evaluated whether the fragment end sequences were also

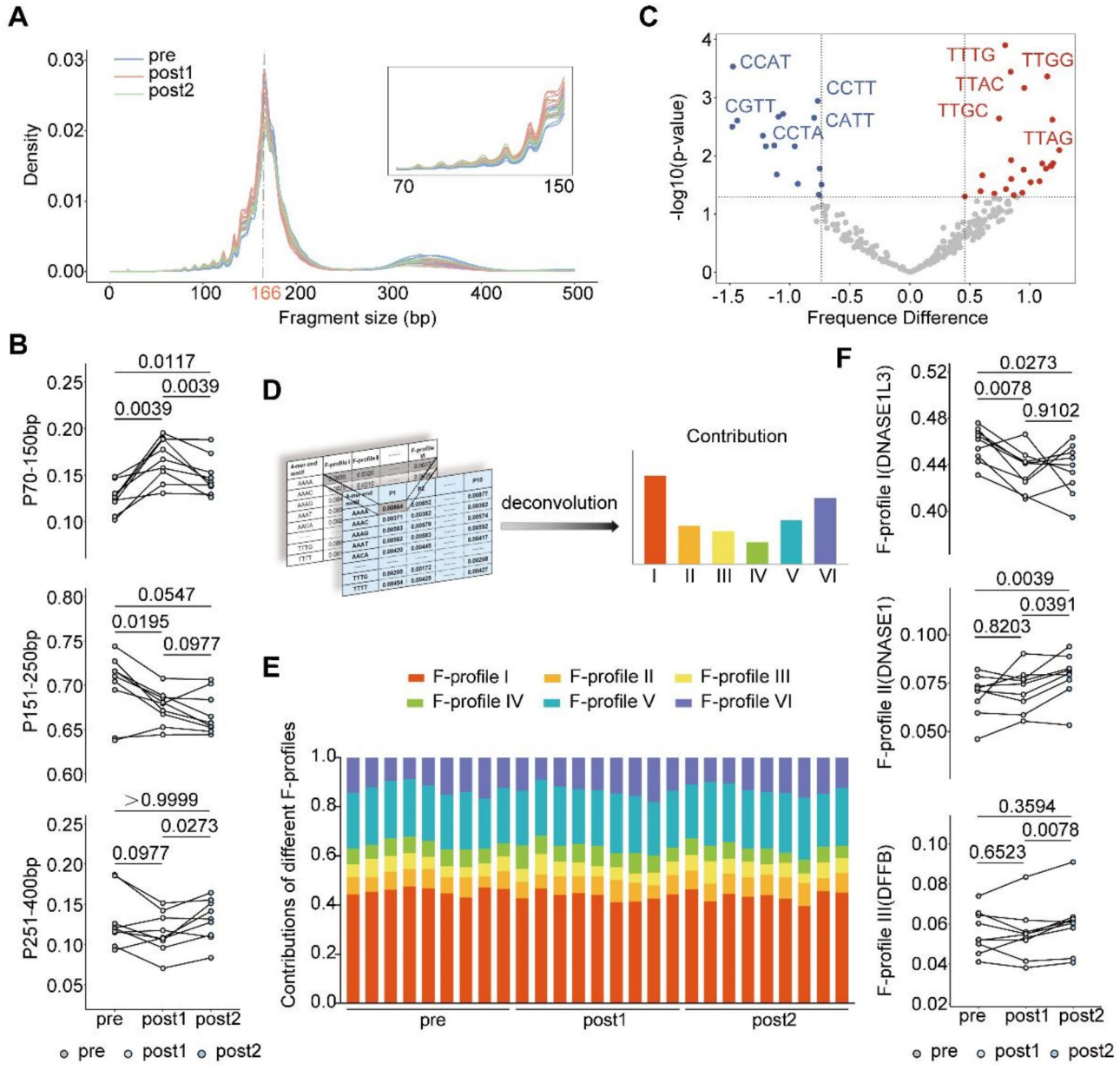

Fig. 2 Profiles of cfDNA fragment size and end motifs. (**A**) Comparison of the fragment size distribution of different groups, which all peaked at 166 bp. Pre: fasting state, post1: 30 min after the meal, post2: 2 h after the meal; (**B**) Comparison of the differences in the proportion of fragment size ranges of 70–150 bp, 151–250 bp, and 251–400 bp between different groups. P values for paired Wilcoxon tests for paired linkage plots are provided; (**C**) Differentially enriched end motifs 30 min after meals compared with fasting state. (**D**) General scheme of NNLS analysis for the 4-mer end-motif profiles. (**E**) Results of end motif deconvolution analyses of plasma cfDNA from different groups; (**F**) Comparison of F-profile I, F-profile II, and F-profile III levels between different groups. P values for paired Wilcoxon tests for paired linkage plots are provided

affected in the postprandial state. Figure 2C showed over-represented frequencies of TTNN motifs and under-represented motifs of CCNN at 30 min postprandial compared to the fasting state, whereas over-represented frequencies of TGNN and GCNN motifs and under-represented motifs of CTNN at 2 hours postprandial (Supplementary Fig. 4C).

To further characterize the roles of nuclease in shaping the cfDNA fragment, we utilized a deconvolutional algorithm in order to estimate the relative contributions of different nucleases to the cfDNA fragmentation (Fig. 2D and E, Supplementary Table 3). Results revealed a significant decrease in F-profile I levels, which are associated with DNASE1L3, at both 30 min ($P = 0.0078$, paired Wilcoxon test) and 2 h ($P = 0.0273$, paired Wilcoxon test) after the meal compared to the fasting state (Fig. 2F). In contrast, the contributions of F-profile II (related to DNASE1) and F-profile III (related to DFFB)

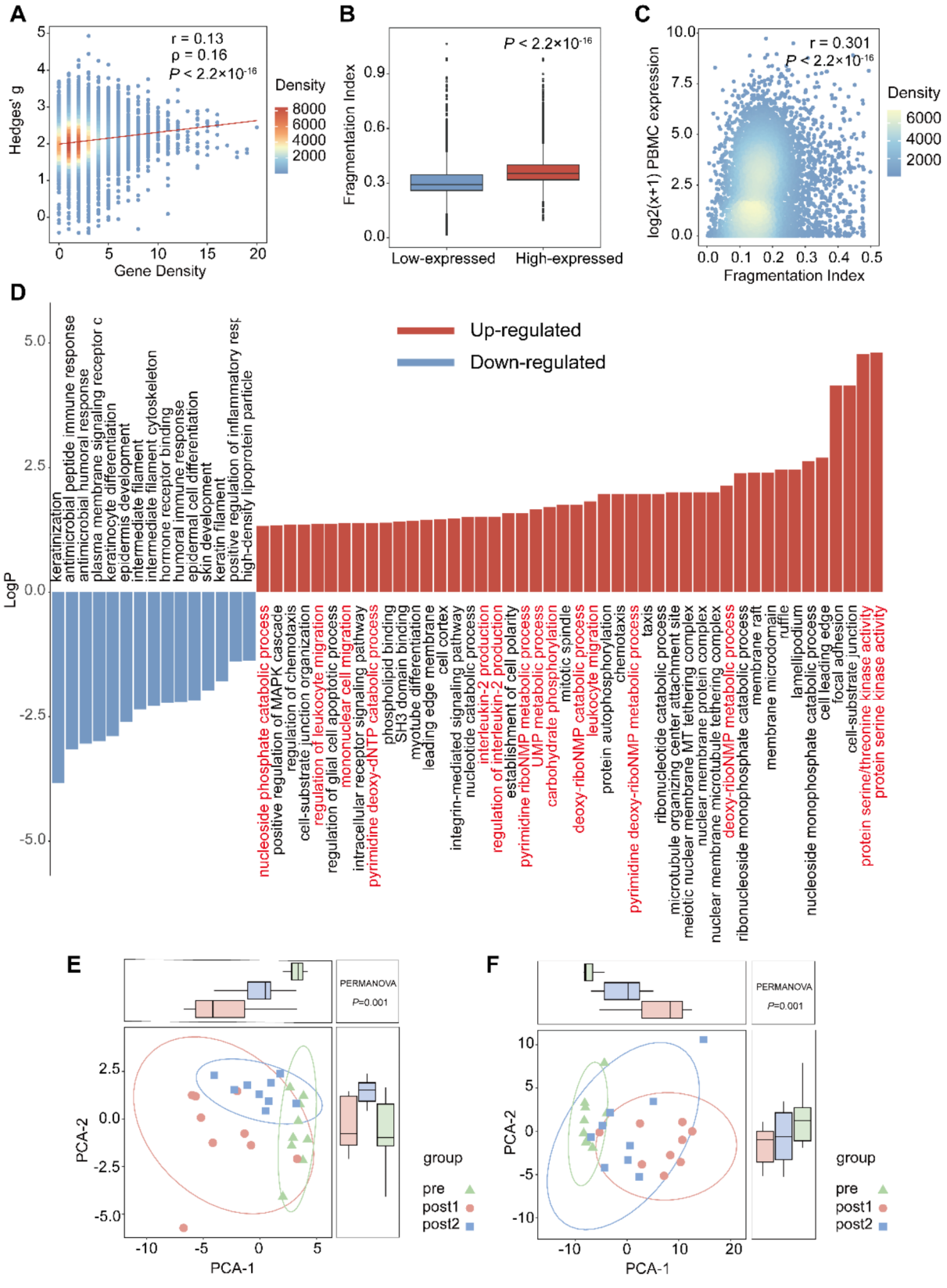

Fig. 3 (See legend on next page.)

(See figure on previous page.)

Fig. 3 Gene expressions inferred by the fragmentation index. (**A**) A scatterplot depicts the relationship between the changes in fragmentation index (Hedges' g) after meals versus gene density. Pearson (r) and Spearman (ρ) correlation coefficients are reported. In both, $P < 2.2 \times 10^{-16}$; (**B**) A box plot of the difference of fragmentation index between low-expressed genes (lower 25% of the total gene) and high-expressed genes (upper 25% of the total gene). P values of the Mann-Whitney U Test comparing the box plot are provided; (**C**) A scatterplot shows a positive correlation between cfDNA fragmentation index from the P5 healthy individual and peripheral blood mononuclear cell RNA expression level (TPM) ($r = 0.301$, $P < 2.2 \times 10^{-16}$, $n = 16{,}157$ genes); (**D**) The bar chart shows the gene enrichment results for 626 up-regulated and 881 down-regulated differentially expressed genes (DEGs) 30 min after a meal. The red-highlighted GO descriptions are related to metabolism and immune processes; PCA plots generated using metabolic (**E**) and immune-related (**F**) DEGs predicted by fragmentation index. PERMANOVA, permutational multivariate analysis of variance

remained relatively stable at 30 min after the meal. However, their contributions significantly increased at 2 h compared with those at 30 min after the meal ($P = 0.0391$ for DNASE1 and $P = 0.0078$ for DFFB, paired Wilcoxon tests) (Fig. 2F). These results were further supported by other studies [33] that the reduction of DNASE1L3 activity will increase short DNA molecules below 120 bp in plasma.

Differentially expressed gene inferred by CfDNA fragmentation

Varieties of physiological changes such as metabolic activity and hormonal responses are associated with meal intake. We thus ought to investigate whether these changes can be reflected in the cfDNA fragmentation patterns. To this end, we used fragmentation index to profile cfDNA fragmentation patterns (see details in method section) on the basis of the fact that cfDNA fragments from expressed genes (that are less protected by nucleosomes) will be more susceptible to cleavage than those from silent genes (that are more protected by nucleosomes) [10, 11]. We first calculated this index in 100 kb bins across the genome, thus obtaining the whole-genome cfDNA fragmentation profile. It revealed a heterogeneous distribution of fragmentation patterns across the entire genome and a significantly positive correlation with gene density (Pearson: 0.13, $P < 2.2 \times 10^{-16}$; Spearman: 0.16, $P < 2.2 \times 10^{-16}$) (Fig. 3A). We further divided the genes into two groups, high-expressed and low-expressed genes, and compared the differences in fragmentation index between the two groups. The results showed that the fragmentation index of high-expressed genes was significantly higher than that of low-expressed genes ($P < 2.2 \times 10^{-16}$, Mann-Whitney U Test) (Fig. 3B). We conducted correlation analyses between the cfDNA fragmentation index and peripheral blood mononuclear cell (PBMC) RNA sequencing data across nine samples. The results revealed a significant positive correlation between the cfDNA fragmentation index and gene expression levels within the gene body, with an average Spearman correlation coefficient of approximately 0.272 (Fig. 3C). To illustrate this trend, we randomly selected one healthy individual's WGS data and corresponding PBMC RNA sequencing data for visualization (Spearman: rho = 0.301, $P < 2.2 \times 10^{-16}$, $n = 16{,}157$ genes) (Fig. 3C). This correlation was further validated using deep WGS data from a patient with CUP and corresponding matched PBMC RNA-seq data (Supplementary Fig. 6A). The correlation was even more significant when the analysis was restricted to gene bodies consisted of at least 500 fragments (Spearman: rho = 0.528, $P < 2.2 \times 10^{-16}$, $n = 4{,}056$ genes). This may be due to a more significant number of cfDNA fragments spanning the gene body, which provides richer information. In comparison, the correlation was lower within 4 kb (2 kb on each side) of the gene transcription start site (TSS) (Spearman: rho = 0.181, $P < 2.2 \times 10^{-16}$, $n = 16{,}139$ genes) (Supplementary Fig. 6B). Additionally, we explored the correlation between the cfDNA fragmentation index and average gene expression across different sequencing depths (50×, 30×, 10×, 5×, 3×, 1×, and 0.5×). The results showed an improved correlation as sequencing depth increased (Supplementary Fig. 6C).

We next attempted to predict the gene expression using the fragmentation index, by employing a Gradient Boosting Machine (GBM) model, and the imputed differentially expressed genes (DEGs) after the meal were analyzed using a non-parameter approach (see details in method section). We identified a total of 626 up-regulated DEGs and 881 down-regulated DEGs when comparing the fasting state to 30 min after the meal, whereas 458 up-regulated DEGs and 981 down-regulated DEGs were found when comparing the fasting state to 2 h after the meal. Subsequently, we performed GO enrichment analyses on these differentially expressed genes to explore changes in gene expression after the meal and their functional significance. The results showed that upregulated genes were primarily enriched in functions related to cell metabolism and immune response, suggesting that changes in postprandial cfDNA fragmentation patterns may be influenced by metabolic adaptation and immune regulation. This finding supports the potential of cfDNA fragmentomics as a biomarker for postprandial metabolic and immune changes. By contrast, downregulated genes were predominantly enriched in functions associated with olfactory perception, cell development and differentiation, and cytoskeletal functions (Fig. 3D, Supplementary Fig. 7, Supplementary Table 4).

To evaluate the dynamic changes of DEGs after meals, we analyzed two groups of genes related to metabolism and immune response from DEGs. The principal component analysis (PCA) results highlighted a distinct

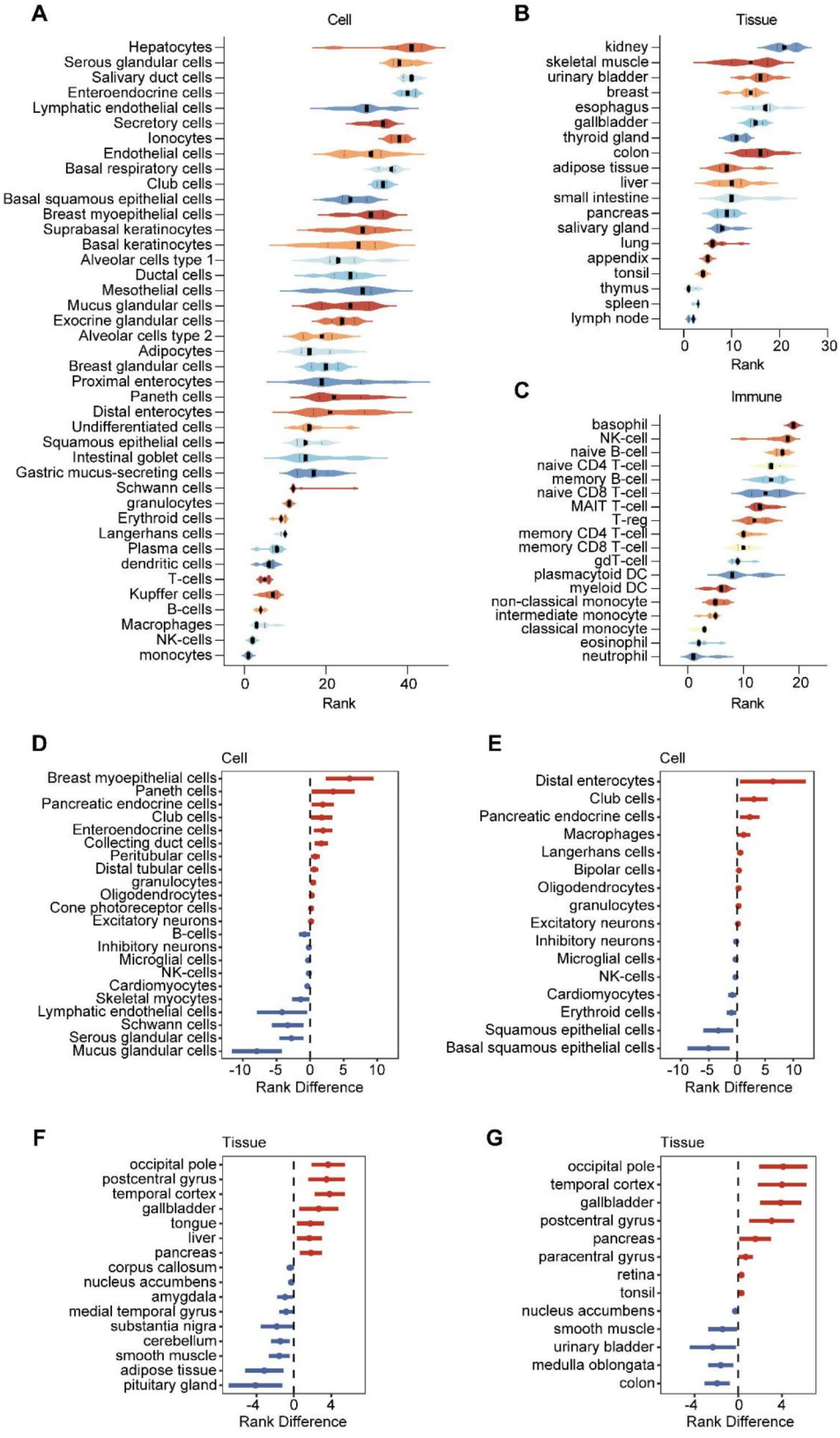

Fig. 4 (See legend on next page.)

(See figure on previous page.)

Fig. 4 Postprandial contributions of cells and tissues to cfDNA inferred from the fragmentation index. The correlation between the fragmentation index of 16,158 gene body regions and the average expression of these genes in 65 cells (**A**) and 51 tissue (**B**) types from the Human Protein Atlas (HPA) database were ranked. (**C**) Ranking of correlations for 18 immune cell types. Violin plots show the distribution of medians (black dots) and quartiles (dotted lines). Cell types with increased (red) or decreased (blue) relative contribution to cfDNA 30 min after a meal (**D**) and 2 h after a meal (**E**). Tissue types with increased (red) or decreased (blue) relative contribution to cfDNA 30 min after a meal (**F**) and 2 h after a meal (**G**). 95% confidence intervals (CI) for sorting differences were estimated using 10,000 bootstrap replicates

DEGs pattern at 30 min after the meal, indicating a significant divergence in metabolism and immune response from the fasting state (Fig. 3E-F, Supplementary Table 4). PERMANOVA analysis confirmed significant differences between groups (*p-value* = 0.001), further supporting the PCA results. In addition, these patterns returned to baseline levels after 2 h, suggesting the temporal and pronounced postprandial effects on gene expression (Fig. 3E-F).

Analysis of postprandial cell and tissue contributions to CfDNA

To investigate the changes of the cell or tissue type composition of cfDNA in the plasma, we correlated the fragmentation index derived from the WGS data with gene expression (nTPM) in 65 cells and 51 tissue types from the Human Protein Atlas (HPA) database. We ranked their relative contributions to cfDNA based on the strength of correlation. This approach helps to perform a comprehensive characterization of plasma cfDNA cell type contributors with great robustness [34]. The results revealed that immune cells contribute most significantly to cfDNA, followed by endothelial, stromal, and epithelial cells (Fig. 4A, Supplementary Table 5). When grouped by tissue type, immune system-associated tissues such as the thymus, lymph node, and spleen ranked the highest (Fig. 4B, Supplementary Table 6). Among immune cell types, monocytes, and lymphocytes were found to contribute the most to cfDNA (Fig. 4C). These results are consistent with previous studies on the cell and tissue type composition of cfDNA in plasma from healthy individuals [34–36]. Moreover, the rankings showed excellent robustness even at a sequencing depth of 0.5 (Supplementary Fig. 8).

We analyzed changes in the relative contributions to cfDNA from various cells or tissues in samples before and after the meal. To account for gender effects, we excluded cells or tissues associated with gender. The results indicated that the relative contributions of cells directly involved in digestion, such as Paneth cells, pancreatic endocrine cells, and enteroendocrine cells (Fig. 4D). We also observed a significant increase in the relative contribution of gastrointestinal tissues such as gallbladder, tongue, liver, and pancreas (Fig. 4F). The use of the deconvolution approach yielded similar results, providing further validation for our observations (Supplementary Fig. 9). These results were in line with our expectations, suggesting that gastrointestinal activity increased after a meal, releasing more cfDNA. Two hours after the meal, as the digestion progressed, the contribution of distal enterocytes to cfDNA became particularly significant (Fig. 4E). Notably, we also found that the relative contribution of immune cells such as macrophages, Langerhans cells, and granulocytes to cfDNA increased significantly, reflecting the enhancement of postprandial immune activity (Fig. 4D and E, Supplementary Table 5).

Furthermore, we detected a significant increase in the contribution of cfDNA from the nervous system, particularly from cells like oligodendrocytes and excitatory neurons, after the meal (Fig. 4D-G). This phenomenon may be attributed to increased neuronal activity and metabolic demand following food intake [37]. The brain plays a central role in regulating energy homeostasis and peripheral metabolism, and postprandial glucose utilization and insulin release have been shown to modulate cortical excitability, which may facilitate cfDNA release from neurons into circulation [38]. Additionally, systemic metabolic shifts may influence blood-brain barrier (BBB) permeability, further promoting the release of cfDNA from neural tissues.

Discussion

Individuals are in a postprandial state for most of the day (16–18 h). However, the impacts of this physiological states on the biological features of cfDNA have not been thoroughly investigated. While there are evidences of a decrease in cfDNA concentration following meals [30], explanations have been limited to potential interference from lipids or proteins in plasma during DNA extraction or the influence of circadian rhythms that may elevate cfDNA levels in the morning. Our prospective study introduces novel observations on how postprandial changes can significantly alter cfDNA fragmentation patterns, offering new insights into the relationship nutritional intake and the profiles of cfDNA as molecular biomarkers.

Our study showed, at the first time, that nucleases played crucial roles in the postprandial effect regarding the changes of cfDNA fragmentation patterns. The enzymatic activity of nucleases, including DFFB, DNASE1, and DNASE1L3, which are integral to the generation and clearance of cfDNA in plasma [4, 39], exhibited significant postprandial fluctuations. We speculated that the enrichment of short DNA molecules in circulation may

be predominantly associated with the reduced activity of DNASE1L3. Previous reports indicated that chromatin is encapsulated in apoptotic microparticles, and the reduction of DNASE1L3 activity increases the exposure of chromatin on the surface of circulating microparticles, which can be protected by forming immune complexes (ICs) with anti-DNA antibodies in plasma [40–42]. This mechanism was also supported by the observation that the amount of short DNA molecules (< 120 bp) exhibited a positive correlation with anti-DNA antibody levels [33]. This increase might be associated with rapid anti-DNA antibody production that protects the short fragments from degradation. Furthermore, DNASE1 was reported to be mainly responsible for the clearance of cfDNA [4], and its increased activity 2 h after the meal can remove cfDNA from plasma, thereby reducing the accumulation of short fragments of cfDNA. While the underlying mechanism regarding the temporal postprandial changes of the nuclease is not yet clear, our study offers a preliminary view into how these changes might be linked to glucose metabolism. DNASE1L3 has been reported to negatively correlate with glycolysis, a key metabolic pathway for glucose utilization [43]. It is possible that the postprandial decrease in DNASE1L3 activity is part of a broader metabolic response to food intake, although this relationship requires further investigation.

We also focused on assessing how food intake affects potential gene expression profiles and the release of cfDNA from cell and tissue sources, using WGS data at low sequencing depths. We found a significant enrichment of genes involved in metabolic processes, cell migration, and cell signaling functions 30 min after a meal based on the predicted gene expression. Moreover, immune and inflammatory responses, such as leukocyte migration, interleukin-2 production, and protein serine kinase activity were also observed after meal. Literature pointed out that postprandial inflammation is mainly caused by the acute rise in circulating triglycerides (TG) [44]. High-fat diets can promote the transfer of endotoxin (lipopolysaccharides) from the gut to the bloodstream, stimulating innate immune cells and causing a transient inflammatory response [45]. Thus, we hypothesized that not only will cells involved in digestion release more cfDNA after a meal, but cfDNA released by immune cells or tissues will also increase. This was subsequently supported by ranking the relative contributions of cells or tissues to cfDNA, which revealed significant increases in the relative contributions of neutrophils, macrophages, and Langerhans cells to cfDNA in plasma after meals.

A primary limitation of our study is the modest sample size. Although we have employed a robust methodology and stringent matching procedures to minimize biological bias, a larger sample would be required to generalize our results to broader populations. Nonetheless, the effect sizes and standard deviations in cfDNA fragmentation that we documented were significant enough to validate the conclusions drawn from our study group (Supplementary Fig. 10). Another important limiting factor is the pre-sampling preparations. Previous studies have reported that acute strenuous exercise can elevate cfDNA concentrations, primarily originating from mature polymorphonuclear neutrophils [46, 47]. Considering this effect, we instructed participants to rest for at least 30 min before fasting blood collection and to remain in a resting state until the final blood draw. However, a 30-minute rest period may still be insufficient to ensure that cfDNA levels return to true baseline levels. To assess the potential impact of exercise on cfDNA changes, we monitored neutrophil levels, but certain limitations remain (Supplementary Table 1). Therefore, future studies should extend the pre-sampling rest period and incorporate other biomarkers to assess the cfDNA baseline level.

Conclusions

In summary, this study offers insights into standardizing preanalytical variables in cfDNA fragmentation analysis and offers new perspectives for understanding metabolic and immune changes at the postprandial state. We observed the impact of postprandial states on cfDNA fragmentation patterns and explored potential mechanisms behind these changes, particularly the role of metabolic and immune factors in them. Our findings suggest that the changes in cfDNA fragmentation are not merely a biological observation but could potentially impact the accuracy and interpretation of non-invasive diagnostic tests that rely on cfDNA analysis. Future studies with larger cohorts will be employed to validate these results and explore their clinical implications further.

Abbreviations

CfDNA	Cell-free DNA
NETosis	Neutrophil extracellular trap
BMI	Body mass index
Kcal	Kilocalorie
EDTA	Ethylenediaminetetraacetic acid
CBC	Complete blood count
BWA	Burrows-wheeler alignment tool
BAM	Binary alignment/map
GC	Guanine and cytosine
LOESS	Locally weighted scatterplot smoothing
F-profiles	cfDNA fragmentation patterns
NNLS	Non-negative least squares
CUP	Cancer of Unknown Primary
GBM	Gradient boosting machine
DEGs	Differentially expressed genes
HPA	The human protein atlas public database
TSV	Tab-separated values
nTPM	Normalized transcripts per million
PERMANOVA	Permutational multivariate analysis of variance
DNASE1L3	Deoxyribonuclease 1 like 3, nuclease
DNASE1	Deoxyribonuclease 1, nuclease
DFFB	DNA fragmentation factor subunit beta, nuclease
WGS	Whole genome sequencing

PBMC	Peripheral blood mononuclear cell
TSS	Transcription start site
GO	Gene ontology
PCA	Principal component analysis

Supplementary Information

The online version contains supplementary material available at https://doi.org/10.1186/s40246-025-00739-4.

Supplementary Table 1

Supplementary Table 2

Supplementary Table 3

Supplementary Table 4

Supplementary Table 5

Supplementary Table 6

Supplementary Figures

Acknowledgements
Not applicable.

Author contributions
Z.T.Z contributed to the methodology, conducted the investigation, performed the formal analysis, and was involved in writing the original draft as well as reviewing and editing the manuscript. T.C was responsible for the methodology, participated in the investigation, and contributed to both writing the original draft and reviewing and editing the manuscript. M.T.Z was involved in the methodology and investigation, conducted the formal analysis, and assisted in reviewing and editing the manuscript. X.D.S contributed to the methodology and participated in formal analysis. P.Y contributed to the methodology, participated in the formal analysis, was involved in reviewing and editing the manuscript, and provided funding for the project. J.A.L was part of the team that developed the methodology. X.Z.D was instrumental in the conceptualization of the study and secured funding for the project. Z.H.T played a key role in the conceptualization of the study, acquired funding, and provided supervision throughout the project. X.C.W was also crucial in conceptualizing the study and acquiring funding.

Funding
This work has been supported by National Natural Science Foundation of China (No.81902156, 82402707), Zhejiang Provincial Natural Science Foundation of China (No. LQ21H160016) and the "Pioneer" and "Leading Goose" R&D Program of Zhejiang Province (No. 2023C03082).

Data availability
Raw sequencing data and the programming codes for the bioinformatics pipeline of this study are available from the corresponding author upon reasonable request.

Declarations

Ethics approval and consent to participate
The study protocol was approved by the Human Ethics Review Committee of the second affiliated hospital of Zhejiang University (2024LSYD0962), and written informed consent was obtained from all subjects before their involvement in the study by the tenets outlined in the Declaration of Helsinki.

Consent for publication
Not applicable.

Competing interests
The authors declare no competing interests.

Author details
[1]Department of Laboratory Medicine, The Second Affiliated Hospital of Zhejiang University, Hangzhou 310009, China
[2]Department of Blood Transfusion, Zhejiang Hospital, Hangzhou 310027, China

Received: 29 December 2024 / Accepted: 4 March 2025
Published online: 18 March 2025

References

1. Brinkmann V, et al. Neutrophil extracellular traps kill bacteria. Science. 2004;303:1532–5. https://doi.org/10.1126/science.1092385.
2. Heitzer E, Auinger L, Speicher MR, Cell-Free DNA. Apoptosis: how dead cells inform about the living. Trends Mol Med. 2020;26:519–28. https://doi.org/10.1016/j.molmed.2020.01.012.
3. Hu Z, Chen H, Long Y, Li P, Gu Y. The main sources of Circulating cell-free DNA: apoptosis, necrosis and active secretion. Crit Rev Oncol Hematol. 2021;157:103166. https://doi.org/10.1016/j.critrevonc.2020.103166.
4. Han DSC, Lo YMD. The Nexus of CfDNA and nuclease biology. Trends Genet. 2021;37:758–70. https://doi.org/10.1016/j.tig.2021.04.005.
5. Ivanov M, Baranova A, Butler T, Spellman P, Mileyko V. Non-random fragmentation patterns in Circulating cell-free DNA reflect epigenetic regulation. BMC Genomics. 2015;16:S1. https://doi.org/10.1186/1471-2164-16-S13-S1.
6. Chiu RWK, Heitzer E, Lo YMD, Mouliere F, Tsui DW. Y. Cell-Free DNA fragmentomics: the new omics on the block. Clin Chem. 2020;66:1480–4. https://doi.org/10.1093/clinchem/hvaa258.
7. Lo YMD, Han DSC, Jiang P, Chiu RWK. Epigenetics, fragmentomics, and topology of cell-free DNA in liquid biopsies. Sci (New York N Y). 2021;372. https://doi.org/10.1126/science.aaw3616.
8. Lo YM, et al. Maternal plasma DNA sequencing reveals the genome-wide genetic and mutational profile of the fetus. Sci Transl Med. 2010;2:61ra91. https://doi.org/10.1126/scitranslmed.3001720.
9. Liu Y, et al. Abstract 5177: Spatial co-fragmentation pattern of cell-free DNA recapitulates in vivo chromatin organization and identifies tissue-of-origin. Cancer Res. 2019;79:5177–5177. https://doi.org/10.1158/1538-7445.Am2019-5177.
10. Ulz P, et al. Inferring expressed genes by whole-genome sequencing of plasma DNA. Nat Genet. 2016;48:1273–8. https://doi.org/10.1038/ng.3648.
11. Esfahani MS, et al. Inferring gene expression from cell-free DNA fragmentation profiles. Nat Biotechnol. 2022;40:585–97. https://doi.org/10.1038/s41587-022-01222-4.
12. Alig SK, et al. Distinct hodgkin lymphoma subtypes defined by noninvasive genomic profiling. Nature. 2024;625:778–87. https://doi.org/10.1038/s41586-023-06903-x.
13. Snyder MW, Kircher M, Hill AJ, Daza RM, Shendure J. Cell-free DNA comprises an. -Of-Origin Cell. 2016;164:57–68. https://doi.org/10.1016/j.cell.2015.11.050. Vivo Nucleosome Footprint that Informs Its Tissues.
14. Liu Y. At the Dawn: cell-free DNA fragmentomics and gene regulation. Br J Cancer. 2022;126:379–90. https://doi.org/10.1038/s41416-021-01635-z.
15. Michaël N, et al. DNA methylation and gene expression as determinants of genome-wide cell-free DNA fragmentation. Nat Commun. 2024;15. https://doi.org/10.1038/s41467-024-50850-8.
16. Derek W, et al. Cell-free DNA from germline TP53 mutation carriers reflect cancer-like fragmentation patterns. Nat Commun. 2024;15. https://doi.org/10.1038/s41467-024-51529-w.
17. Taylor R. Early detection of malignant and pre-malignant peripheral nerve tumors using cell-free DNA fragmentomics. Clin Cancer Res. 2024. https://doi.org/10.1158/1078-0432.ccr-24-0797.
18. Yuying H, Xiang-Yu M, Xionghui Z. Systematically evaluating Cell-Free DNA fragmentation patterns for Cancer diagnosis and enhanced Cancer detection via integrating multiple fragmentation patterns. Adv Sci (Weinh). 2024;11. https://doi.org/10.1002/advs.202308243.
19. Peter J. Clinical validation of a cell-free DNA fragmentome assay for augmentation of lung cancer early detection. Cancer Discov. 2024. https://doi.org/10.1158/2159-8290.cd-24-0519.
20. Spencer C. Jagged ends on multinucleosomal Cell-Free DNA serve as a biomarker for nuclease activity and systemic lupus erythematosus. Clin Chem. 2022;68. https://doi.org/10.1093/clinchem/hvac050.
21. Ze Z, et al. Jagged ends of urinary Cell-Free DNA: characterization and feasibility assessment in bladder Cancer detection. Clin Chem. 2021;67. https://doi.org/10.1093/clinchem/hvaa325.

22. Peiyong J, et al. Preferred end coordinates and somatic variants as signatures of Circulating tumor DNA associated with hepatocellular carcinoma. Proc Natl Acad Sci USA. 2018;115. https://doi.org/10.1073/pnas.1814616115.
23. van der Pol Y, et al. The effect of preanalytical and physiological variables on Cell-Free DNA fragmentation. Clin Chem. 2022;68:803–13. https://doi.org/10.1093/clinchem/hvac029.
24. Hu X, et al. Effects of blood-processing protocols on cell-free DNA fragmentomics in plasma: comparisons of one- and two-step centrifugations. Clin Chim Acta. 2024;560:119729. https://doi.org/10.1016/j.cca.2024.119729.
25. Meessen ECE, Warmbrunn MV, Nieuwdorp M, Soeters MR. Human postprandial nutrient metabolism and Low-Grade inflammation: A narrative review. Nutrients. 2019;11. https://doi.org/10.3390/nu11123000.
26. Sasso E, Baticic L, Sotosek V. Postprandial dysmetabolism and its medical implications. Life (Basel). 2023;13. https://doi.org/10.3390/life13122317.
27. Hotamisligil GS. Inflammation and metabolic disorders. Nature. 2006;444:860–7. https://doi.org/10.1038/nature05485.
28. Ning F, et al. Cardiovascular disease mortality in Europeans in relation to fasting and 2-h plasma glucose levels within a normoglycemic range. Diabetes Care. 2010;33:2211–6. https://doi.org/10.2337/dc09-2328.
29. Zitvogel L, Pietrocola F, Kroemer G. Nutrition, inflammation and cancer. Nat Immunol. 2017;18:843–50. https://doi.org/10.1038/ni.3754.
30. Poulet G, et al. Circadian rhythm and Circulating cell-free DNA release on healthy subjects. Sci Rep. 2023;13:21675. https://doi.org/10.1038/s41598-023-47851-w.
31. Zhou Z, et al. Fragmentation landscape of cell-free DNA revealed by deconvolutional analysis of end motifs. Proc Natl Acad Sci USA. 2023;120:e2220982120. https://doi.org/10.1073/pnas.2220982120.
32. Cook L, et al. Does size matter?? Comparison of extraction yields for different-Sized DNA fragments by seven different routine and four new Circulating Cell-Free extraction methods. J Clin Microbiol. 2018;56. https://doi.org/10.1128/JCM.01061-18.
33. Serpas L, et al. Dnase1l3 deletion causes aberrations in length and end-motif frequencies in plasma DNA. Proc Natl Acad Sci U S A. 2019;116:641–9. https://doi.org/10.1073/pnas.1815031116.
34. Stanley KE, et al. Cell type signatures in cell-free DNA fragmentation profiles reveal disease biology. Nat Commun. 2024;15:2220. https://doi.org/10.1038/s41467-024-46435-0.
35. Moss J, et al. Comprehensive human cell-type methylation atlas reveals origins of Circulating cell-free DNA in health and disease. Nat Commun. 2018;9:5068. https://doi.org/10.1038/s41467-018-07466-6.
36. Loyfer N, et al. A DNA methylation atlas of normal human cell types. Nature. 2023;613:355–64. https://doi.org/10.1038/s41586-022-05580-6.
37. Bruning JC, Fenselau H. Integrative neurocircuits that control metabolism and food intake. Science. 2023;381:eabl7398. https://doi.org/10.1126/science.abl7398.
38. Chen W, Cai W, Hoover B, Kahn CR. Insulin action in the brain: cell types, circuits, and diseases. Trends Neurosci. 2022;45:384–400. https://doi.org/10.1016/j.tins.2022.03.001.
39. Han DSC, et al. The biology of Cell-free DNA fragmentation and the roles of DNASE1, DNASE1L3, and DFFB. Am J Hum Genet. 2020;106:202–14. https://doi.org/10.1016/j.ajhg.2020.01.008.
40. Sisirak V, et al. Digestion of chromatin in apoptotic cell microparticles prevents autoimmunity. Cell. 2016;166:88–101. https://doi.org/10.1016/j.cell.2016.05.034.
41. Pisetsky D. The role of microparticles in the pathogenesis of SLE: a new look at an old paradigm. Lupus Sci Med. 2017;4:e000220. https://doi.org/10.1136/lupus-2017-000220.
42. Radic M, Marion T, Monestier M. Nucleosomes are exposed at the cell surface in apoptosis. J Immunol. 2004;172:6692–700. https://doi.org/10.4049/jimmunol.172.11.6692.
43. Xiao Y, et al. Deoxyribonuclease 1-like 3 inhibits hepatocellular carcinoma progression by inducing apoptosis and reprogramming glucose metabolism. Int J Biol Sci. 2022;18:82–95. https://doi.org/10.7150/ijbs.57919.
44. Mazidi M, et al. Meal-induced inflammation: postprandial insights from the personalised responses to dietary composition trial (PREDICT) study in 1000 participants. Am J Clin Nutr. 2021;114:1028–38. https://doi.org/10.1093/ajcn/nqab132.
45. Fritsche KL. The science of fatty acids and inflammation. Adv Nutr. 2015;6:S293–301. https://doi.org/10.3945/an.114.006940.
46. Atamaniuk J, et al. Increased concentrations of cell-free plasma DNA after exhaustive exercise. Clin Chem. 2004;50:1668–70. https://doi.org/10.1373/clinchem.2004.034553.
47. Fridlich O, et al. Elevated CfDNA after exercise is derived primarily from mature polymorphonuclear neutrophils, with a minor contribution of cardiomyocytes. Cell Rep Med. 2023;4:101074. https://doi.org/10.1016/j.xcrm.2023.101074.

Publisher's note